INTRODUCTION OF A DUAL INJECTION TUBE FOR THE DESIGN OF A 20 MW LEAD-BISMUTH TARGET SYSTEM

Chung-Ho Cho, Yonghee Kim, Tae-Yung Song
Korea Atomic Energy Research Institute
150 Duckjin-Dong, Yuseong, Daejeon, 305-353 Korea

Abstract

A spallation target system is a key component in the development of an accelerator-driven system (ADS). It is known that a 15-25 MW spallation target is required for a practical 1 000 MWth ADS. The design of a 20 MW spallation target is very challenging because more than 60% of the beam power is deposited as heat in a small volume of the target system. In the present work, a numerical design study was performed to obtain the optimal design parameters of a 20 MW spallation target for a 1 000 MWth ADS. A dual injection tube was proposed for the reduction of the LBE flow rate at the target channel. The results of the present study show that a 30-cm wide proton beam with a uniform beam distribution should be adopted for the spallation target of a 20 MW power. When the dual LBE injection tube is employed, the LBE flow rate is reduced by a factor of four without reducing the maximum allowable beam current.

Introduction

In an ADS a high-energy proton beam is impinged on a heavy metal target to produce spallation neutrons that are multiplied in a subcritical blanket. Therefore, the spallation target is one of the most important units of an ADS. Lead-bismuth eutectic (LBE) is preferred as the target material due to its high neutron production rate, effective heat removal and a very small amount of radiation damage properties. In addition, it can be used simultaneously as a reactor coolant.

The key issue in the target design is how to design an appropriate beam window and LBE flow so that the system can sustain thermal and mechanical loads as well as radiation damage. Recently, there have been some intensive studies on the design of LBE spallation targets [1,2]. It is well known that a proton beam power of 15-25 MW is required for a practically sized (~1 000 MWth power) ADS [3]. The design of a 20 MW spallation target is very challenging because more than 60% of the beam power is deposited as heat on the window and in a small volume of the target system [4].

Due to the difficulties of designing high-power targets, a three-beam target system was proposed by Forschungszentrum Karlsruhe; the target designs without beam windows are also considered in the MYRRHA project and the X-ADS design [5,6,7]. Although these proposals have some preferable characteristics for high-power targets, they still have some difficulties in other aspects when compared to the more typical LBE target designs (i.e. a single beam with a solid window).

The main objective of the present paper is to show the possibility of designing a 20 MW LBE spallation target with a beam window. In a previous study, we designed a 20 MW LBE target for HYPER [8]. However, it was found that the LBE flow rate was too high at almost 10% of the total coolant flow rate, and the average LBE temperature rise in the target outlet was too low compared to the LBE heat-up in the core. These problems result in an increased pumping power of the coolant, potential thermal striping of the core upper structures and a decrease in the thermal efficiency of the system. Thus, it is essential to reduce the LBE flow rate in the target channel without hampering the target performance.

For this purpose, we introduce a dual LBE injection tube (DIT), which controls the LBE velocity distribution at the target inlet. Sensitivity studies for the DIT have been performed for the HYPER target system and the results are provided in this paper.

Target system

The Korea Atomic Energy Research Institute (KAERI) has been developing an ADS called HYPER [10]. HYPER is a 1 000 MWth fast spectrum reactor with $k_{eff} = 0.98$ and is designed to transmute the TRU, Tc-99 and I-129 coming from PWRs. HYPER is expected to need a 19 mA proton beam of 1 GeV to sustain the 1 000 MWth power level.

LBE is the target material and the target coolant. The beam window material is 9Cr-2WVTa. It is advanced ferritic-martensitic steel that is known to be more resistant to LBE corrosion than austenitic steels and does not show a ductile-to-brittle transition temperature (DBTT) problem while being resistant to radiation damage [11].

The cylindrical beam tube and hemi-spherical beam window are adopted in the basic target design of HYPER. Although hexagonal fuel assemblies surround the LBE flow channel, the target channel is assumed to have a cylindrical shape for the thermal-hydraulic calculation of the target channel. Figure 1 shows the reference target system schematically. The beam window diameter (D_w) and the beam window thickness are 35 cm and 2.0 mm, respectively. The target channel diameter (D_t)

is set at 66 cm. The beam diameter (D_b) should be as large as possible since a larger beam diameter means a smaller beam current density, which makes the peak temperature lower. There should be a minimum distance between the beam tube and the beam. But, since the proton beam may shift from its original axis, the minimum distance between the beam tube and the beam is 0.5 cm larger than a proton beam shift distance, or $D_w - D_b = 5$ cm. Two alternative radial distributions of the proton beam current density (uniform and parabolic distributions) are considered in the thermal-hydraulic analysis.

The LBE inlet temperature (T) is the same as the inlet temperature of the core coolant, 340°C. The pressure load, which is applied to the beam tube located 10 cm above the junction point of the beam tube and the beam window, is assumed to be 16 atm. LBE inlet velocity (V) can be adjusted locally by using orifices, although the flow is connected to the core coolant LBE.

The first criteria are the maximum allowable velocity and the temperature of the LBE. The erosion and corrosion rates of the structural material are increased as the LBE velocity and temperature increase. Therefore, the velocity of the LBE is fixed at 500°C and 2 m/s [12]. The second set of criteria are the maximum allowable temperature and the stress of the beam window. Steels are usually degraded significantly if the temperature is too high. Therefore, 600°C is chosen as the maximum allowable temperature for the beam window. The stress intensity of the beam window is not allowed to exceed 1/3 of the yield strength of 9Cr-2WVTa [13]. The yield strength of 9Cr-2WVTa is 480 MPa at 600°C, which means the maximum allowable stress is 160 MPa [14].

Figure 1. The reference target system

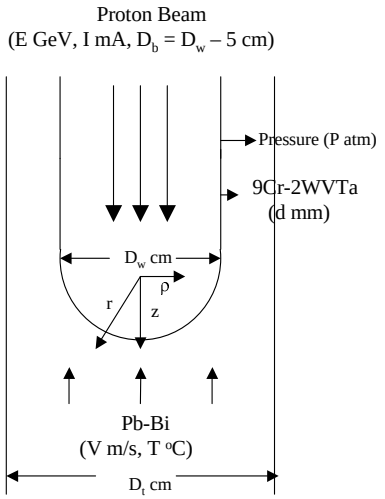

Numerical simulation

The material data for the calculation are listed in Table 1. The data used for the LBE and 9Cr-2WVTa are values at 450°C and 500°C, respectively. Since the data used for 9Cr-2WVTa are not available, the data of 9Cr-MoVNb except for yield strength are used. Due to the two being ferritic 9Cr steels, the thermal expansion coefficient, density and thermal conductivity are not very different.

Table 1. Material data used for calculations

LBE (450°C)	Density (10.2 g/cm^3) Thermal conductivity (14.2 W/m·K) Thermal expansion coeff. (1.2×10^{-4} K^{-1}) Viscosity (1.39 centipoise)	9Cr-2WVTa (500°C)	Density (7.6 g/cm^3) Thermal conductivity (30 W/m·K) Thermal expansion coeff. (1.23×10^{-5} K^{-1})

The heat generation inside the beam window and the LBE is calculated using the LCS 2.7 (LAHET code system) [15]. The thermal-hydraulic analyses of the target system are performed using the CFX 4.4 code. In the thermal-hydraulic analyses, all the calculations were performed using the standard k-ε turbulence model to predict the turbulent flow characteristics, and the logarithmic law of the wall to predict the near-wall characteristics. Sufficient mesh refinement is used in each case to obtain y+ values between 30 and 200 in the heated regions, indicating that the turbulence model can provide reasonable predictions in these regions. The calculation is performed as a steady state simulation using the SIMPLEC solution algorithm and upwind differencing scheme. Also, the thermal-hydraulic behaviour is evaluated using an axi-symmetric model. The maximal uniform inlet velocity of the LBE is decided based on the criterion that the LBE velocity at the target system does not exceed 2 m/s. Figure 2 contains a schematic of the computational domain and the adopted boundary conditions.

Figure 2. The computational domain and the BC

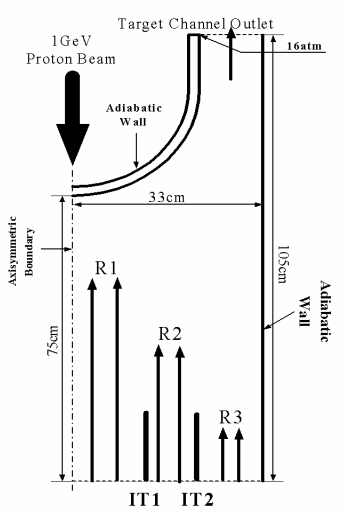

Heat generation

The heat generation inside the beam window and LBE is calculated using the LCS 2.7 for the two types of proton beam distributions – uniform and parabolic distributions. The results of the LCS are fitted to obtain the current density functions, which express the heat generation rates with a variable proton beam current.

1. A parabolic distribution is as follows:

$$Q = C\frac{2I}{\pi R_b^4}(R_b^2 - \rho^2) \qquad \text{unit: W/cm}^3 \tag{1}$$

2. A uniform distribution is as follows:

$$Q = CI \qquad \text{unit: W/cm}^3 \qquad (2)$$

where I = proton beam current (mA), R_b = beam radius (cm), ρ = distance from the centre (cm) and C = fitted coefficient.

First, thermal-hydraulic analyses of the reference target system were performed to compare the two beam profiles, uniform and parabolic, under the same calculation conditions. The LBE inlet velocity was 1.31 m/s and the beam current was 20.0 mA. The peak temperatures of the LBE with a parabolic and uniform beam distribution were 654°C and 505°C, respectively. In addition, the peak temperatures of the beam window with the parabolic and the uniform distribution were 736°C and 547°C, respectively. Clearly, the uniform beam distribution provides a lower peak temperature. In the same case, the allowable beam currents satisfying the design criteria with a parabolic and a uniform distribution were calculated to be 10.1 mA and 19.3 mA, respectively. All the cases show that the allowable beam current is constrained by the peak temperature of the LBE, 500°C, not by the peak temperature of the beam window, 600°C. In the case of the uniform beam distribution, the allowable beam currents were 19.3 mA, which is about twice that of the parabolic beam profile case.

Consequently, the uniform beam target system was adopted for HYPER. However, this target system has two unfavourable features: 1) LBE flow rate (4 562 kg/s) is almost 10% of that of the active core (45 506.26 kg/s) and 2) average LBE exit temperature (356°C) is too low when compared to the core average coolant temperature of 490°C. The large flow rate in the target channel increases the pumping power and the temperature difference between the target coolant and the core coolant may cause the so-called thermal striping behaviour. Thus, it is highly desirable that the LBE flow rate be minimised, while keeping the maximum proton beam.

For a comparison, we analysed the target with an LBE flow rate reduced by 50%. In this case, the maximum beam currents satisfying the design criteria with parabolic and uniform distributions were calculated to be 5.4 mA and 10.1 mA, respectively. The target system with a reduced flow rate does not offer a sufficient beam current to sustain the 1 000 MWth power level of the HYPER.

Effect of single injection tube

The lesser the flow rate of the target channel, the lesser the allowable beam current; thus, it is difficult for the present target system to reduce the flow rate with a sufficient beam current to sustain the 1 000 MWth power level of HYPER. As a result, a cylindrical injection tube (IT), which is located in the centre of a target channel, was introduced to reduce the flow rate in the target system.

In order to investigate the effect of the single injection tube (SIT), thermal-hydraulic analyses were performed with the two types of proton beam distributions with a beam current of 20 mA. The SIT diameter and the SIT height were 31 cm and 10 cm, respectively, and the thickness of the IT was 2 mm. Due to the proton beam diameter being 30 cm, the SIT diameter was wider than that of the proton beam to avoid any direct irradiation of the proton beam at the SIT. The LBE inlet velocity at the target channel without SIT was 0.655 m/s. The LBE inlet velocities of R1 and R2 (+R3) were 1.5 m/s and 0.417 m/s, respectively.

Figure 3 shows the temperature distributions of the wetted surface at the beam window with/without the SIT. Without the SIT, the peak temperature of the wetted surface at the beam window is 928°C for the parabolic beam and 657°C for the uniform beam. With the SIT, the peak temperature of the wetted surface at the beam window is 652°C with the parabolic beam and 515°C with the uniform beam. With the SIT, the peak temperature of the wetted surface at the beam window is significantly reduced.

Figure 3. Temperature distributions of the wetted surface at the beam window

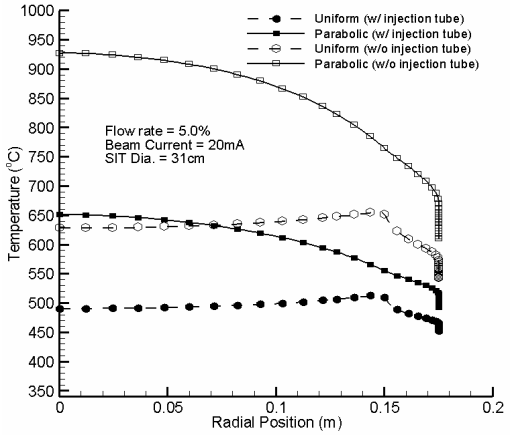

For the SIT concept, thermal-hydraulic analyses were performed to determine the maximum beam current satisfying the design criteria. The LBE inlet velocities of R1 and R2 (+R3) were 1.635 m/s and 0.378 m/s, respectively. The maximum beam currents satisfying the design criteria with the parabolic and the uniform beam distributions were calculated to be 10.3 mA and 19.6 mA, respectively. The results show that the introduction of an SIT is a good counterproposal to reduce the flow rate of the target system with a sufficient beam current to sustain the 1 000 MWth power level of the ADS.

In order to investigate the effect of a variation in the SIT diameter, thermal-hydraulic analyses were performed. The diameter of the SIT was varied from 10 cm to 35 cm and the SIT height was fixed at 10 cm. The LBE inlet velocity of R1 was fixed at 1.5 m/s and the LBE inlet velocity of R2 (+R3) was decided based on the flow rate of the target system not exceeding 5.0% of that of the active core. The proton beam current was 20 mA. Figure 4 shows the temperature distributions of the wetted surface at the beam window with the SIT diameter variation. In the case of the uniform beam, the wider the diameter of the SIT, the greater the cooling effect at the beam window. In the case of the parabolic beam, the narrower the diameter of the SIT, the greater the cooling effect at the beam window.

In order to investigate the changes of temperature and velocity distribution in the target system with flow rate variations, thermal-hydraulic analyses were performed. The SIT diameter and height were fixed at 10 cm. Beam currents of the parabolic and uniform beams were 12.3 mA and 19.6 mA, respectively. While the LBE inlet velocity of R1 was fixed at 1.95 m/s, the flow rate of R2 (+R3) was reduced little by little. The flow rate of R1 was 156 kg/s, or 0.34% of that of the active core.

The peak temperature at the beam window and the LBE with the flow rate variation is shown in Table 2. The temperature distributions of the wetted surface at the beam window are shown in Figure 5. Although the total flow rate of the target channel was reduced to 2.8% of that of the active core, in the case of the parabolic beam, the changes of the peak temperature were very small. But, in the case of the uniform beam, the changes of the peak temperature with the flow rate variation were larger than that of the parabolic beam. When the LBE inlet velocity of R2 (+R3) was 0.62 m/s, the peak temperature of the LBE of the wetted surface at the beam window met the design criterion. In the

case of the parabolic beam, the peak temperature of the wetted surface at the beam window gradually shifted outwards from the centre of the beam window along the beam window surface, which was contrary to the typical temperature distribution at the beam window surface with a parabolic beam. In the case of the uniform beam, the peak temperature of the beam window occurred near the intersection of the proton beam boundary with the beam window and increased with the flow rate reductions.

Figure 4. Temperature distributions of the wetted surface at the beam window with the SIT diameter variation

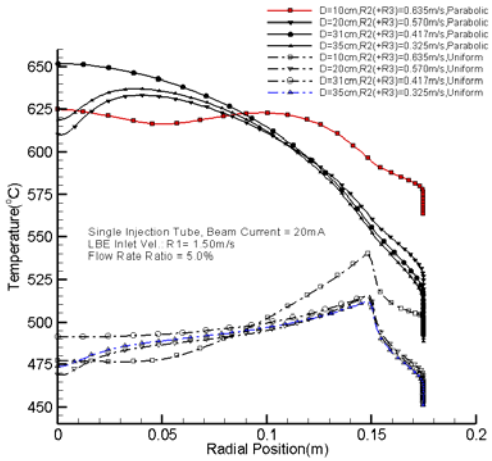

Table 2. Peak temperature of the beam window and the LBE with flow rate reduction

LBE inlet velocity of R2 (+R3) (m/s)		0.62	0.5	0.4	0.3	0.25
Total flow rate ratio of target channel (%)		5.0	4.07	3.33	2.57	2.21
Parabolic	Peak temp.(beam window, inner surface, °C)	529	528	527	526	525
	Peak temp.(beam window, wetted surface, °C)	479	478	478	481	483
Uniform	Peak temp.(beam window, inner surface, °C)	540	544	550	558	562
	Peak temp.(beam window, wetted surface, °C)	500	505	511	518	523

Figure 5. Temperature distribution of the wetted surface at the beam window with the flow rate reduction

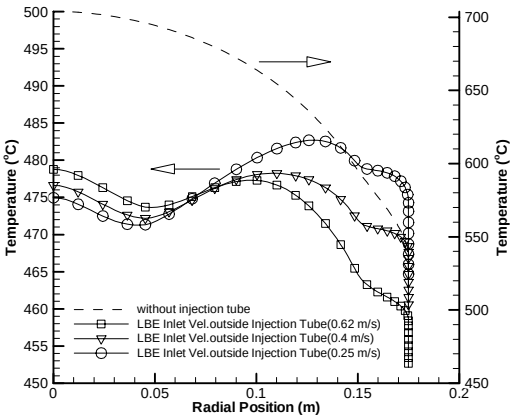

(a) Parabolic beam

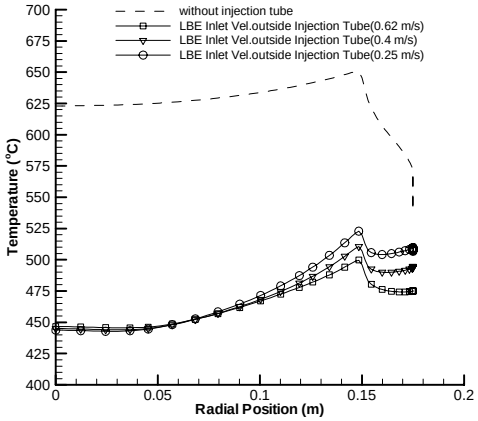

(b) Uniform beam

Figure 6. The velocity and temperature distribution in the target channel with flow rate variations

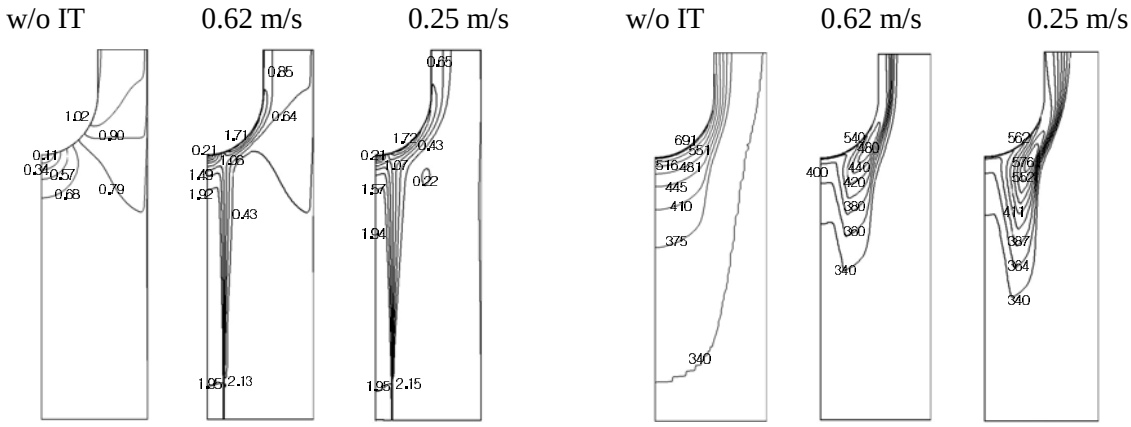

Figure 6 shows the velocity and the temperature distribution in the target system with the flow rate reduction of R2 (+R3). Due to the relatively high velocity of the LBE of R1, the flow stagnation region existing below the beam window centre was substantially decreased. But, with the injection tube, another flow stagnation region developed below 45° from the beam window centre when the flow rate of R2 (+R3) was reduced substantially. It caused a temperature increase of the LBE near the intersection of the proton beam boundary with the beam window, and the peak temperature of the LBE occurred at the thermal island in the flow field of the LBE.

Effect of dual injection tube

It is clear that the target system with an SIT offers not only a more allowable beam current but also a significantly reduced flow rate at the target channel. However, when an SIT is employed, a new flow stagnation region develops below the beam window with the flow rate reductions. It causes a temperature increase of the LBE near the intersection of the proton beam boundary with the beam window. In addition, with the SIT concept, the LBE flow rate could not be further reduced without reducing the maximum allowable beam current. Therefore, we introduced a dual injection tube (DIT), which provides a greater degree of freedom in the LBE flow field control.

Table 4. Parameter sets of DIT

Case 1	Case 2	Case 3	Case 4
D1 = 10 cm, D2 = 30 cm	D1 = 10 cm, D2 = 35 cm	D1 = 20 cm, D2 = 30 cm	D1 = 20 cm, D2 = 35 cm

In order to investigate the effect of DIT, thermal-hydraulic analyses were performed with a fixed flow rate of the target system, 5% of that of the active core, and the results are shown in Figure 7. There are four kinds of DIT as shown in Table 4. The LBE inlet velocities of R1 and R2 were 1.95 m/s and 1.0 m/s, respectively. The beam currents of the parabolic beam and the uniform beam were 12.3 mA and 19.6 mA, respectively.

In Figure 7, in all cases except Case 1, a drop in temperature occurred at the beam window centre. In the case of the uniform beam, the wider the diameter of the inner IT (IT1), the greater the cooling effect at the beam window. In the case of the parabolic beam, the smaller the diameter of the inner IT

(IT1), the greater the cooling effect at the beam window. The results showed that Case 1 with the parabolic beam and Case 3 with the uniform beam would be the optimum parameter set from the viewpoint of the peak temperature at the beam window.

Figure 7. Temperature distributions of the wetted surface at the beam window with DIT diameter variations

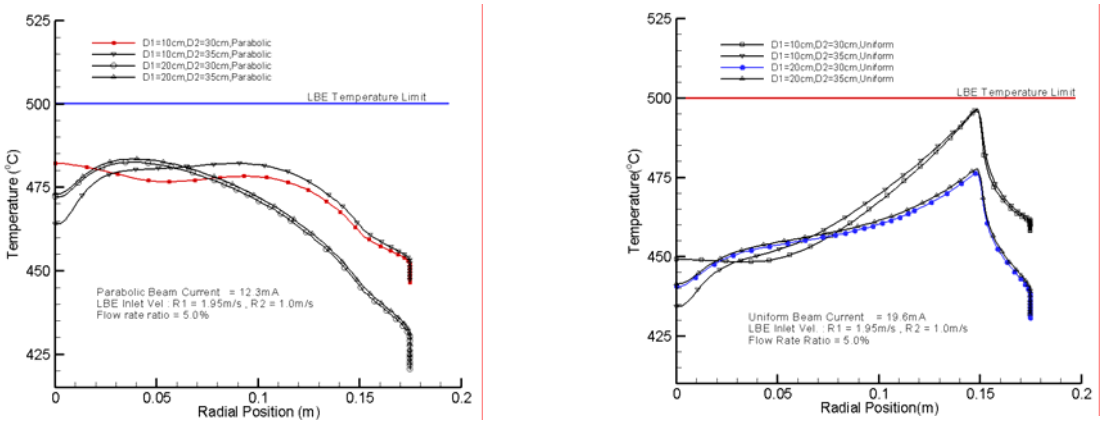

(a) Parabolic (b) Uniform

In order to investigate the changes of the temperature distribution at the beam window with the flow rate variations, thermal-hydraulic analyses were performed with Case 1 and Case 3 (results are shown in Figures 8 and 9). The beam currents of the parabolic and the uniform beam profile were 12.3 mA and 19.6 mA, respectively. The LBE inlet velocities of R1 for Case 1 and Case 3 were 1.95 m/s and 1.80 m/s, respectively. While the LBE inlet velocity of R3 was fixed at 0.2 m/s, the flow rate of R2 was reduced little by little.

Figure 8. The temperature distributions of the wetted surface at the beam window with the parabolic beam

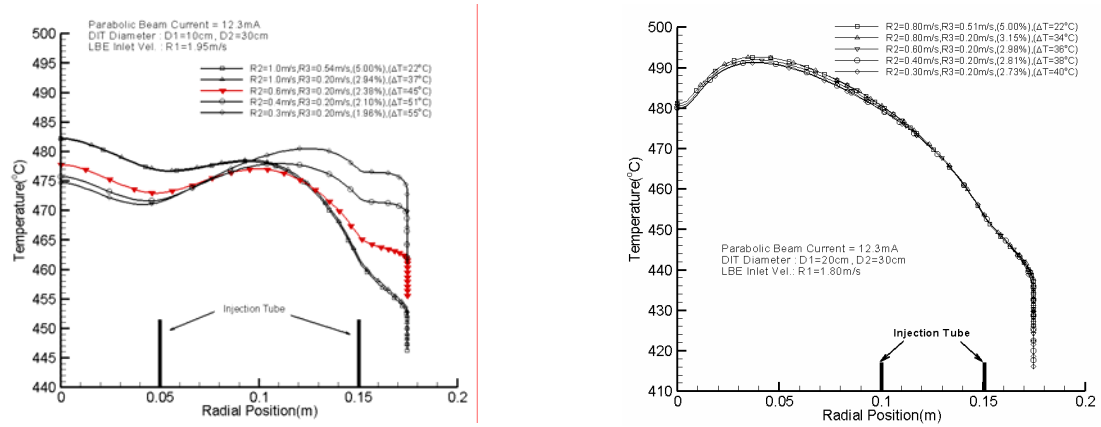

(a) Case 1 (b) Case 3

In Figure 8, Case 1 was more effective for beam window cooling than Case 3. In the case of R2 = 0.3m/s, the LBE flow rate of the target channel could be reduced by a factor of five with an increased allowable maximum beam current (14.0 mA) and an average LBE exit temperature (395°C). In the case of R2 = 0.6 m/s, which would be the optimum case from the viewpoint of the peak temperature at the beam window, the allowable maximum beam current was 14.28 mA.

As shown in Figure 9, Case 3 was more effective for the beam window cooling than Case 1. Also, the temperature increases of the wetted surface at the beam window with the flow rate reductions were smaller than with Case 1 or the SIT. The results showed that a new flow stagnation region, which developed below the beam window, was very well controlled by the DIT. In the case of R2 = 0.3 m/s, the LBE flow rate of the target channel could be reduced by a factor of four with an increased allowable maximum beam current of 21.27 mA and an average LBE exit temperature of 398°C.

Figure 9. Temperature distributions of the wetted surface at the beam window with the uniform beam

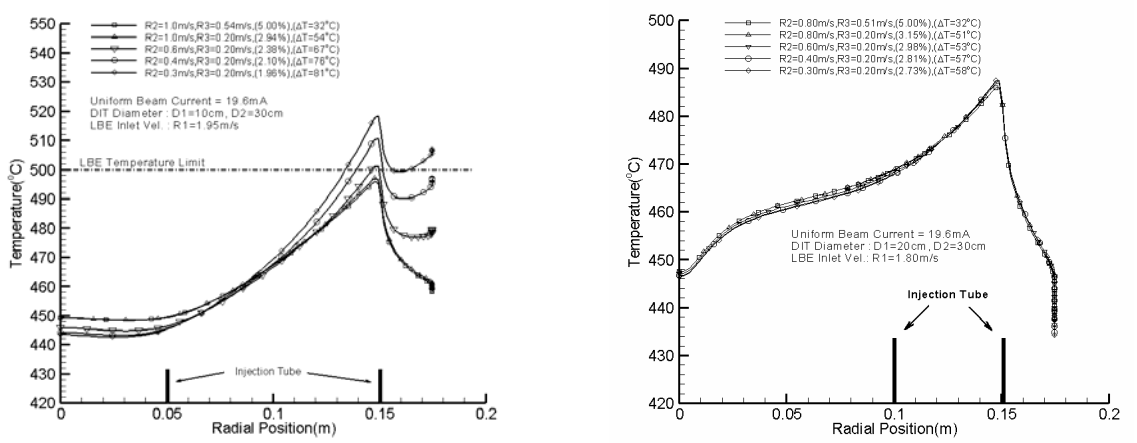

(a) Case 1 (b) Case 3

Conclusions

In this paper, a cylindrical injection tube, which is located in the centre of a target channel, was introduced to reduce the flow rate at the target system.

With a dual injection tube having a 10 cm inner tube diameter and a 30 cm outer tube diameter, the allowable maximum beam current was 14.0 mA for a parabolic beam, which was ~159% higher than that of the target system without an injection tube. In addition, with a dual injection tube having a 20 cm inner tube diameter and a 30 cm outer tube diameter, the allowable maximum beam current was 21.27 mA for a uniform beam, which was ~111% higher than that of the target system without an injection tube. From the viewpoint of thermal-hydraulics, the results show that a smaller diameter of the inner injection tube would be appropriate for the parabolic beam and a wider diameter of the inner injection tube would be appropriate for the uniform beam.

The results indicated that the target system with a dual injection tube offers not only a higher allowable beam current but also a significantly reduced flow rate at the target channel. If the inlet velocity of R3 was further reduced, the LBE flow rate could be decreased without reducing the maximum allowable beam current (currently being tested in a related study).

Acknowledgements

The Korean Ministry of Science and Technology (MOST) provided support for this work.

REFERENCES

[1] Buono, S., *et al*., "Numerical Studies Related to the Design of the Beam Target of the Energy Amplifier Prototype", Heavy Liquid Metal Conference 1998, Vol. 1, pp. 249 (1998).

[2] Cheng, X., I. Slessarev, "Thermal-hydraulic Investigations on Liquid Metal Target System", *Nuclear Engineering and Design*, 202, 297-310 (2000).

[3] Kim, Y.H., *et al*., "Optimisation of Height-to-diameter Ratio for an Accelerator-driven System", *Nuclear Science and Engineering*, Vol. 143, pp. 141-157 (2003).

[4] Tak, N.I., *et al*., "Numerical Studies on Thermal Hydraulics of HYPER Target", AccApp & ADTTA '01, Reno, Nevada, 11-15 November 2001.

[5] Cheng, X., *et al*., "Thermal Hydraulic Design of an ADS with Three Spallation Targets", *Proceedings of ADTTA '99*, Prague, Czech Republic (1999).

[6] Tichelen, K.V., *et al*., "MYRRHA Project, a Windowless ADS Design", *Proceedings of ADTTA '99*, Prague, Czech Republic (1999).

[7] Ansaldo, "XADS Pb-Bi Cooled Experimental Accelerator Driven System Reference Configuration", Summary Report (2001).

[8] Cho, C.H., T.Y. Song, N.I. Tak, "Numerical Design of a 20 MW Lead–Bismuth Spallation Target for an Accelerator-driven System", *Nuclear Engineering and Design*, Vol. 229, pp. 317-327 (2004).

[9] Park, W.S., *et al*., Development of Nuclear Transmutation Technology, KAERI/RR-1702/96 (1997).

[10] Dai, Y., "Martensitic/ferritic Steels as Container Materials for Liquid Mercury Target of ESS", *Proceedings of the International Workshop on the Technology and Thermal Hydraulics of Heavy Liquid Metal*, 6.27-6.39 (1996).

[11] Yachmenyov, G.S., *et al*., "Problems of Structural Materials' Corrosion in Lead-Bismuth Coolant", *Proceedings of Heavy Liquid Metal Coolants in Nuclear Technology*, Vol. 1, pp. 133-140 (1999).

[12] Rust, J.H., *Nuclear Power Plant Engineering*, Haralson Publishing Company, pp. 385 (1979).

[13] Klueh, R.L., "Experience with Ferritic/Martensitic Steels for Fusion Application", *Proceedings of International Workshop on Spallation Materials*, 3.3-3.26 (1996).

[14] Prael, R.E., *et al*., *User Guide to LCS: The LAHET Code System*, LA-UR-89-3014, Los Alamos National Lab (1989).

TABLE OF CONTENTS